



# Antioxidant Potential of *Tisochrysis lutea* through Urea-Based Nanonutrient Enrichment: Experimental Modeling and Computational Approach

Ayoub Ainane<sup>1</sup>, Fatouma Mohamed Abdoul-Latif<sup>2\*</sup>, Laila Achenani<sup>1</sup>,  
Ali Merito Ali<sup>2</sup>, Houda Mohamed<sup>2,3</sup>, Ahmad Abu Arra<sup>4</sup>, Stefano  
Cacciatore<sup>5</sup>, Tarik Ainane<sup>1</sup>

<sup>1</sup>Superior School of Technology, University of Sultan Moulay Slimane, BP 170, Khenifra  
54000 Morocco.

<sup>2</sup>Medicinal Research Institute, Center for Research and Study of Djibouti, BP 486, Djibouti.

<sup>3</sup>Peltier Hospital of Djibouti, Djibouti City P.O. Box 2123, Djibouti.

<sup>4</sup>Department of Civil Engineering, Yildiz Technical University, 34220 Istanbul, Türkiye.

<sup>5</sup>Bioinformatics Unit, International Centre for Genetic Engineering and Biotechnology  
(ICGEB), Cape Town 7925, South Africa

*Tisochrysis lutea* is a marine microalga of the Haptophyta family, widely exploited in aquaculture due to its diverse chemical composition and potential in bioactive compounds, including its antioxidant activity. In this study, the antioxidant potential of *T. lutea* culture enriched with different urea-based nanonutrients (urea, methylurea, tetramethylurea, cyanoguanidine, and diurethane dimethacrylate) was evaluated using DPPH, FRAP and ICA methods revealing a general benefit from using urea-based nanonutrients. Chemical profiles indicated increased contents of total carotenoids and polyphenols. Correlations between antioxidant profile, chemical composition, and molecular descriptors were determined using statistical approaches such as principal component analysis (PCA) and multiple linear regression (MLR). Molecular docking confirmed specific and stable interactions between urea and its derivatives with key proteins in nitrogen management. The results demonstrated that urea-based nanonutrients significantly enhance the production of bioactive metabolites in *T. lutea*, thus offering promising prospects for biotechnological applications.

**Keywords:** Antioxidant profiles; Chemical composition; Correlation; molecular

descriptors; molecular docking; *Tisochrysis lutea*.

## **1. Introduction**

Microalgae constitute a valuable renewable resource with the potential to replace conventional industrial production of fossil fuel-derived chemicals [1]. The microalgae cultivation industry provides significant and high-quality added value, meeting the demands of industrial applications, particularly in agri-food and pharmaceutical technologies [2-3]. Microalgae biomass contains carotenoids, polyphenols, and other biomolecules widely used as dietary supplements [4-6].

Secondary metabolites of microalgae, such as carotenoids, polyphenols, and polysaccharides, are attracting increasing interest in scientific and industrial fields [7]. Carotenoids, notably fucoxanthin, and astaxanthin, have powerful antioxidant properties, contributing to photoprotection and the prevention of chronic diseases, which makes them valuable in nutraceuticals and cosmetics [8-9]. Polyphenols, known for their antioxidant and antimicrobial effects, are being explored for pharmaceutical and food applications [10]. They protect cells from oxidative damage and have therapeutic potential for various diseases. Polysaccharides, conversely, have immune-stimulating and thickening properties, making them useful in the pharmaceutical and food industries [11]. They can improve the texture of foods, act as controlled release agents in pharmaceutical formulations, and strengthen the immune system. However, microalgae biomass production, cultivation methods, variations in culture media composition, and protocols for chronological monitoring of nutrient contents constitute the main obstacles to the large-scale commercialization of this emerging bio-industry [12-13].

Optimization of microalgae metabolic pathways through modification of the culture medium and/or nutrients represents a powerful tool for physiological control, generally more feasible than direct metabolic modification [14]. Visions for adjusting nutrient-driven biomass composition are typically cost-effective, environmentally friendly, broadly applicable, and adaptable to various microalgae species of industrial interest. Processes such as nutrient limitation or starvation can be easily programmed and optimized to achieve high productivity levels for desired target compounds. These strategies are currently used to induce the overproduction of metabolites such as lipids, polysaccharides, and pigments [15].

To this end, microalgae, particularly *Tisochrysis lutea* of the Haptophytes division, occupy an essential place in algal biotechnology, particularly as food for vertebrate larvae [16]. This species stands out as the most promising producer of the dominant carotenoid, fucoxanthin, which accounts for up to 98% of its total carotenoid content [17]. Furthermore, *T. lutea* is a significant producer of various secondary metabolites, thus reinforcing its industrial interest. The development of culture conditions is fundamental for biotechnological processes, particularly for *T. lutea*. Although this species is cultivated on a small scale, it is more often exploited on a large scale. Various modifications of culture media have been developed, particularly concerning nutrient compositions, thereby improving biomass yield and promoting a high content of active biomolecules [18].

On the other hand, several studies highlight the importance of nitrogen as an essential nutrient for microalgae growth [19-20]. Nitrogen promotes increased biomass production, as

well as a notable increase in chlorophyll and carotenoid contents [21]. As a primary macronutrient, nitrogen plays a central role in synthesizing proteins, lipids, and carbohydrates in microalgae. The nitrogen concentration significantly influences the growth of microalgae and their biochemical composition [22]. Concomitantly, nitrogen depletion in the culture medium results in reduced growth but a concomitant increase in lipid productivity. Microalgae can assimilate nitrogen in the form of nitrate, nitrite, urea, and ammonium. Nitrate is generally preferred for microalgae cultivation over ammonium salts because it is more stable and has less chance of pH fluctuation. Additionally, ammonium ( $\text{NH}_4^+$ ) concentrations above 25  $\mu\text{M}$  are toxic to microalgae, which explains why nitrate ( $\text{NO}_3^-$ ) is commonly used. However, limiting nitrogen in the culture medium could reduce biomass production while increasing lipid production [23-25].

The impact of urea on microalgae cultivation has been further explored in several recent studies, highlighting its effects on secondary metabolite production. As a nutrient source, urea has several significant advantages for microalgae cultivation. Its use is economically beneficial by reducing process costs while providing ecological benefits by reducing environmental impacts related to nitrates and ammonium. It thus constitutes a sustainable alternative for the production of valuable metabolites. Research by Nwoye Eze et al. (2020) [26] showed that adding urea to a mixotrophic *Desmodesmus subspicatus* medium significantly increased the simultaneous production of carotenoids and lipids. Urea optimization increased carotenoid concentration and lipid yields, illustrating its effectiveness in producing high-value bioproducts. Similarly, Minyuk et al. (2020) [27] observed that urea can replace nitrate in the cultivation of carotenogenic microalgae without negatively affecting carotenoid production. Urea substantially increased lipid yields while maintaining the levels of valuable carotenoids, such as astaxanthin and canthaxanthin. Furthermore, Molina-Miras et al. (2023) [28] revealed that urea can replace nitrate and ammonium in the cultivation of *Amphidinium carterae*, promoting growth equivalent to that observed with nitrate. Furthermore, urea enhanced the production of some secondary metabolites, such as amphidinol, and enhanced the antiphytopathogenic activity. Also, Martins Rosa et al. (2023) [29] demonstrated that urea, as a carbon and nitrogen source, enhances the photosynthesis and growth of *Chlamydomonas reinhardtii* under mixotrophic conditions, leading to enhanced biomass production and increased photosynthetic rates.

This work, aimed at treating *T. lutea* cultures enriched with nitrogen compounds, in particular urea-based nanonutrients such as urea, methylurea, tetramethylurea, cyanoguanidine, and diurethane dimethacrylate, by in vitro and in silico evaluation of the antioxidant potential and its correlation with secondary metabolites and computational descriptors, aims to:

- (1) Evaluate the antioxidant potential of *T. lutea* cultures enriched with urea-based nanonutrients.
- (2) Determine the chemical composition in secondary metabolites of *T. lutea* cultures enriched with urea-based nanonutrients.
- (3) Establish correlations between antioxidant activities and secondary metabolites of *T. lutea*.

- (4) Analyze correlations with computational descriptors via *in vivo* and *in silico* experiments.
- (5) Use statistical tools such as principal component analysis (PCA) and multiple linear regression (MLR) to identify significant relationships.
- (6) Confirm by molecular docking the specific and stable interactions between urea and its derivatives with proteins essential for nitrogen management.

## **2. Material and methods**

### **2.1. Algal growth**

The microalgae studied, *T. lutea*, were provided by the strain library of the Institut de Recherche Médicinale (CERD, Djibouti), with an initial origin from Tadjoura, Djibouti (N1°46'58.084", E42°53'1.667"). The culture medium used was the f/2 medium of Guillard and Ryther (1962), prepared from filtered and sterilized seawater. Six culture conditions were set up: a control condition and five others with the addition of molecules at a concentration of 250 nM, namely urea **A**, methylurea **B**, tetramethylurea **C**, cyanoguanidine **D**, and diurethane dimethacrylate **E** (Figure S1), hence, all compounds used were of high quality. The cultures were carried out in 2-liter glass Schott bottles, with a culture volume of 2 liters for each bottle. Light intensity was maintained at 50  $\mu\text{mol m}^{-2} \text{s}^{-1}$  using LED panels, and a 12h:12h light-dark cycle was applied. The temperature was controlled at  $20 \pm 1$  °C, and aeration of 0.2 L  $\text{min}^{-1}$  with filtered air (0.22  $\mu\text{m}$ ) was ensured. As inoculum, initial cultures of 50–100 mL in exponential growth phase were used, with an initial density of  $5.0 \times 10^5$  cells  $\text{mL}^{-1}$  for *T. lutea*. The experiment was conducted for a period of 15 days. Cell abundance was determined using a CytoFLEX flow cytometer (Beckman Coulter, USA), and cultures were performed in triplicate for each experimental condition [30-32].

### **2.2. Extraction procedure**

The extraction process was carried out using the maceration method. To do this, 1 gram of *T. lutea* microalgae was extracted with 100 mL of a solvent composed of hexane, methanol, and chloroform, in a volumetric ratio of 1:2:2. This operation was carried out overnight at room temperature, protected from light. The extraction was repeated in triplicate to ensure complete extraction, and all obtained extracts were amalgamated. The combined extracts were filtered through Whatman No. 4 filter paper to remove solid particles. The concentration of the extracts was carried out by vacuum evaporation using a rotary evaporator, allowing the removal of residual solvents. The concentrated extracts were preserved in amber glass vials and stored at -20 °C until further use. This procedure ensures the preservation of the bioactive compounds in the microalgae, thus facilitating their analysis and use in subsequent studies [33].

### **2.3. Antioxidant activity**

Several specific methods were used to evaluate the antioxidant activity, including the 1,1-diphenyl-2-picrylhydrazyl (DPPH) radical decolorization assay, the ferric reducing antioxidant power (FRAP) assay, and the iron chelating activity (ICA) assay.

The DPPH radical test was used to quantify the free radical scavenging activity [34]. To do this, 25  $\mu\text{L}$  of the sample or Trolox standard solution was placed in an ELISA microplate reader (Thermo Scientific, Multiskan 60, Waltham, MA, USA). Then, 75  $\mu\text{L}$  of a 4 mM methanolic DPPH solution was added. The plate was kept in the dark at room temperature for half an hour, and then the absorbance was measured at 540 nm. Trolox was used as a reference in this assay. Antioxidant activity was determined by the percentage of radical scavenging using the following equation:

$$\% \text{RSA} = \left( A_{\text{blank}} - \frac{A_{\text{sample}} - A_{\text{control}}}{A_{\text{blank}}} \right) \times 100 \quad (1)$$

Based on the Trolox calibration curve, the results were expressed as mg Trolox equivalent per gram of dry biomass (mg TE  $\cdot\text{g}^{-1}$  DW).

The FRAP assay was performed to measure the ability of antioxidants to reduce the 2,4,6-tripyridyl-s-triazine- $\text{Fe}^{3+}$  complex ( $[\text{Fe}(\text{TPTZ})_2]^{3+}$ ) to its ferrous equivalent  $[\text{Fe}(\text{TPTZ})_2]^{2+}$  [35]. For this purpose, 20  $\mu\text{L}$  of the sample (or Trolox standard solution) was added to an ELISA microplate reader, followed by the incorporation of 180  $\mu\text{L}$  of FRAP reagent. This reagent was freshly prepared with 300 mM sodium acetate/acetic acid buffer, 10 mM TPTZ in 40 mM HCl, and 20 mM ferrous chloride hexahydrate in a ratio of 10:1:1, respectively. The plate was incubated at 37  $^{\circ}\text{C}$  for 5 minutes, after which the absorbance was measured at 595 nm. Referring to the Trolox calibration curve, the results were expressed as mg Trolox equivalents (TE) per gram dry biomass (DW).

The iron chelating activity (ICA) assay was performed by adapting a recognized method with some adjustments [36]. For this analysis, 120  $\mu\text{L}$  of the sample was placed in a 96-well microtiter plate, followed by the addition of 60  $\mu\text{L}$  of 2 mM iron (II) chloride. Incorporation of 40  $\mu\text{L}$  of 5 mM ferrozine solution initiated the reaction, forming a ferrozine- $\text{Fe}^{2+}$  complex responsible for the magenta coloration. The color produced was measured after 30 minutes at 540 nm. EDTA- $\text{Na}_2$  was used as a positive standard. The results were expressed as percentage of ICA and calculated according to the following equation:

$$\% \text{ICA} = \left( A_{\text{blank}} - \frac{A_{\text{sample}} - A_{\text{control}}}{A_{\text{blank}}} \right) \times 100 \quad (2)$$

#### 2.4. Secondary metabolite quantification

Quantification of secondary metabolites was performed using four distinct analytical methods, thus allowing a comprehensive assessment of the composition of the microalgae obtained after each culture in terms of carotenoid, total phenolic, and total carbohydrate content. This multidimensional approach ensured a detailed characterization of the metabolites essential for the study while providing valuable information on their antioxidant potential.

Carotenoid content was determined using an adapted method, as described by Liang et al. (2023) [37]. Samples were extracted with methanol, and filtered, and the filtrate was separated with petroleum ether. After the removal of residual water, the volume was adjusted with ethanol, and the absorbance was measured at 450 nm to quantify carotenoids.

Total phenolic compound (TPC) content was assessed using a modified Folin-Ciocalteu *Nanotechnology Perceptions* Vol. 20 No.4 (2024)

method described by Sanou et al. (2023) [38]. Gallic acid was used as a standard, and calibration curves were established with concentrations ranging from 0 to 500 mg/L. Samples were mixed with Folin-Ciocalteu solution and sodium carbonate, and then incubated in the dark for one hour. Absorbance measured at 765 nm allowed quantification of TPC, expressed as milligrams of gallic acid equivalent per gram of dry matter.

Finally, the free carbohydrate content was determined following a modified method for the quantification of sugars, as described by Rašeta et al. (2024) [39]. To do this, 50  $\mu\text{L}$  of a 4% phenol solution and 250  $\mu\text{L}$  of concentrated sulfuric acid were added to 100  $\mu\text{L}$  of sample or standard solution. After a 10-minute incubation at room temperature, the absorbance was measured at 490 nm. Based on a glucose standard curve, total carbohydrate concentration was calculated and expressed as milligrams of glucose equivalent (GluE) per gram of dry matter.

## 2.5. Bioinformatics modeling

In this study, bioinformatics modeling was performed using two distinct analytical approaches to gain an in-depth understanding of the mechanisms involved in the antioxidant potential of the compounds and their interactions with key proteins in nitrogen metabolism.

### 2.5.1. Quantitative Analysis of Structure and Antioxidant Potential

The first approach was to establish a quantitative relationship between the chemical structure of compounds A, B, C, D, and E and their antioxidant potentials using QSAR (Quantitative Structure-Activity Relationship) modeling [40-41]. This method involved using various molecular descriptors to characterize the properties of the compounds and understand the mechanisms underlying their antioxidant activity [42].

The molecular descriptors were classified as follows:

- **Physicochemical descriptors:** They include the molecular formula, molecular weight, and the percentages of elements such as carbon (C%), hydrogen (H%), nitrogen (N%), and oxygen (O%). These parameters, such as molar volume, molar refractive power, density, surface tension, and polarizability, provide information about molecules' size, shape, and potential interactions.
- **Topological Descriptors:** Including the Balaban index, cluster count, and topological indices such as the Wiener Index and topological diameter. These descriptors assess the connectivity and structure of molecules, helping to understand their complexity and overall properties.
- **Electronic descriptors:** They include  $E_{\text{HOMO}}$ ,  $E_{\text{LUMO}}$  and  $E_{\text{GAP}}$  which are respectively the energy of the highest occupied molecular orbital, the energy of the lowest unoccupied molecular orbital and the energy gap. These descriptors provide essential information on the chemical reactivity and electronic stability of molecules. From these parameters, other properties such as chemical hardness ( $\eta$ ), electronegativity ( $\chi$ ) and electrophilicity index ( $\omega$ ) have been determined.

- **Molecular Dynamics Descriptors:** These include molecular flexibility (S) and shape coefficient, which help to understand the dynamics of molecules and their ability to adopt different conformations.

The chemical structures of the compounds were drawn with ChemBiodraw Ultra, and energy was minimized using the MMFF94 model in ChemDraw 3D. The descriptors were calculated and were presented in Table S2 [43].

### 2.5.2. Molecular Screening of Protein-Ligand Interactions

The second approach consisted of a molecular screen to evaluate the interactions between the five compounds and proteins essential for nitrogen management and fixation in various organisms, including microalgae. Three selected proteins, available in the RCSB database (PDB identifiers: 1LLW, 2MH7, 7U6O), were chosen for their relevance in the study of interactions with antioxidant compounds. Protein structures were prepared using BIOVIA Discovery Studio Visualizer to remove heteroatoms, cocrystallized ligands, and solvents to perform this analysis. Autodock 4 and Autogrid 4 tools were used to assign polar charges and generate optimized pdbqt files. Compounds were drawn with ChemDraw Ultra, energetically minimized with Chem 3D Pro, and then converted to pdbqt format via OpenBabel. Virtual screening was performed with Autodock 4, and ligand-protein interactions were visualized and analyzed with BIOVIA Discovery Studio Visualizer. Ligand poses were validated by calculating the root mean square deviation (RMSD), ensuring values below 2.0 for ligands re-docked by co-crystallization. This approach allowed us to determine the specific interactions between compounds and proteins, contributing to a detailed understanding of the potential effects of these compounds in the targeted metabolic processes [44-45].

### 2.6. Statistical studies

Statistical approaches were employed in this study to model and understand the complex relationships between the biological properties of the compounds and their molecular characteristics, thus providing an in-depth view of their antioxidant potential as well as their interaction with various experimental factors, both in vivo and in silico.

In the first, values were obtained from three replicates for each assay to ensure the accuracy of the results. Statistical analysis of numerical data was performed using Type A uncertainty assessment, and tests were subjected to Student's t-test ( $p < 0.05$ ) to determine their significance.

An analysis of variance (ANOVA) was applied to identify significant differences between groups of samples, followed by Tukey's test. This multiple test detected significant variations between groups and provided a detailed assessment of the differences.

Correlations between variables were examined using principal component analysis (PCA) and multiple linear regression (MLR). These methods were used to establish relationships between the antioxidant profile and two sets of variables: on the one hand, the composition of the biomolecules (such as the content of carotenoids, phenolic compounds, and carbohydrates) and, on the other hand, the calculated descriptors. PCA allowed the reduction of the dimensionality of the data by keeping only the most relevant factors and eliminating

those that are highly correlated with each other, thus simplifying the correlation matrix. MLR was used to establish a mathematical relationship between the antioxidant profile and the factors studied, whether they are the metabolite composition or the molecular descriptors. This method assumes a linear relationship between the dependent variable (the antioxidant properties) and the independent variables (the metabolite compositions or the descriptors).

### 3. Results

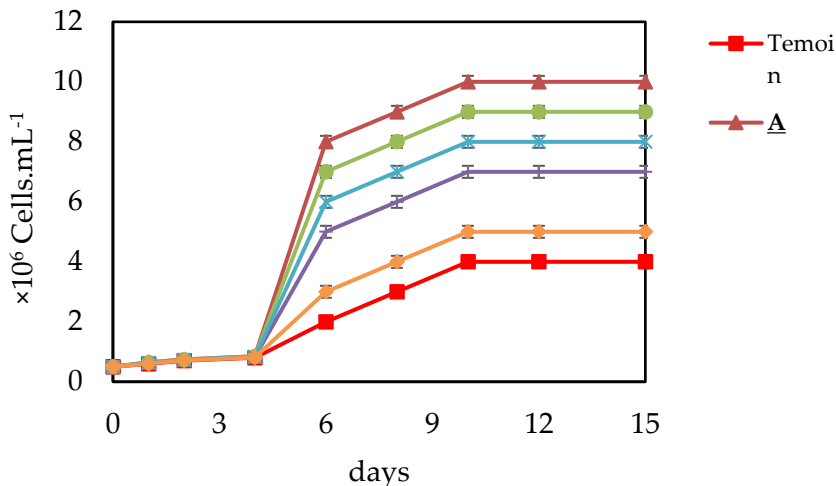
#### 3.1. Microalgae growth

The cultures of *Tisochrysis lutea* microalgae were carried out in different culture media containing nanonutrients (A: Urea, B: Methylurea, C: Tetramethylurea, D: Cyanoguanidine, E: Diurethane dimethacrylate) with a concentration of 250 mM. Table 1 presents the evolution of the number of microalgae cells in these different culture media, as well as a control, over 15 days. All media with urea-based nanonutrients showed an effect on the growth of the strains, which allowed to classify the growth as follows: Urea > Methylurea > Cyanoguanidine > Tetramethylurea > Diurethane dimethacrylate.

Media containing urea and methylurea showed greater growth and reached a higher number of microalgae cells compared to the other media and the control, with  $10 \times 10^6$  cells/mL and  $9 \times 10^6$  cells/mL, respectively. The media with nanonutrients cyanoguanidine and tetramethylurea showed moderate growth, with cell numbers ranging from  $7 \times 10^6$  cells/mL to  $8 \times 10^6$  cells/mL. The medium with nanonutrient E showed slightly lower growth compared to the control, with  $5 \times 10^6$  cells/mL.

The overall results proved the effect of nitrogen-based nanonutrients on the growth of the microalgal strain *T. lutea*.

Figure 1 Growth curves of *T. lutea* cultured with different urea-based nanonutrients.





### 3.2. Antioxidant activity and chemical profiles

A series of maceration extractions were performed after cultivating *T. lutea* microalgae in media enriched with different urea-based nanonutrients. First, the antioxidant activity was measured using three methods (DPPH radical decolorization, FRAP, and ICA). Table 1 presents the results obtained for these antioxidant activities. According to the three methods, all the extracts of the cultures with nanonutrients revealed higher antioxidant activities than the control. The culture extract with urea presented higher values (1.37 mg TE.g<sup>-1</sup> DW according to DPPH, 7.12 mg GAE.g<sup>-1</sup> DW according to FRAP, and 17.41 mg EDTA.g<sup>-1</sup> DW according to ICA). In addition, the extracts from other cultures also showed significant values.

On the other hand, the chemical profiles were established by the quantification of the essential secondary metabolites: total carotenoid content (TCD), total polyphenols content (TPC), and total carbohydrates content (TCC). Table 2 presents the results obtained during the quantification of these secondary metabolites. All microalgae extracts presented higher total carotenoid and polyphenol contents compared to the control, with values ranging from 26.21 mg g<sup>-1</sup> DW to 44.15 mg g<sup>-1</sup> DW for total carotenoids, and from 13.82 mg GAE g<sup>-1</sup> DW to 19.10 mg GAE g<sup>-1</sup> DW for total polyphenols. In contrast, the total carbohydrate content of all microalgae extracts was lower compared to the control, with all values below 31.12 mg GluE.g<sup>-1</sup> DW.

Table 1 Antioxidant activities of *T. lutea* microalgae cultured with different urea-based nanonutrients according to three methods: DPPH radical decolorization assay, the FRAP assay, and the ICA.

Culture	Y1 : DPPH (mg TE .g <sup>-1</sup> DW)	Y2 : FRAP (mg GAE .g <sup>-1</sup> DW)	Y3 : ICA (mg EDTA .g <sup>-1</sup> DW)
Control culture	0.55 ± 0.06 <sup>a</sup>	1.31 ± 0.05 <sup>a</sup>	14.80 ± 0.24 <sup>a</sup>
<u>A</u>	1.37 ± 0.14 <sup>d</sup>	7.12 ± 0.85 <sup>d</sup>	17.41 ± 0.81 <sup>b,c</sup>
<u>B</u>	0.92 ± 0.08 <sup>c</sup>	5.44 ± 0.55 <sup>d</sup>	16.75 ± 0.70 <sup>b</sup>
<u>C</u>	0.70 ± 0.06 <sup>b</sup>	2.18 ± 0.15 <sup>c</sup>	15.98 ± 0.33 <sup>b</sup>
<u>D</u>	0.86 ± 0.09 <sup>c</sup>	2.15 ± 0.15 <sup>c</sup>	16.20 ± 0.74 <sup>b,c</sup>
<u>E</u>	0.63 ± 0.05 <sup>a,b</sup>	1.88 ± 0.05 <sup>b</sup>	15.03 ± 0.38 <sup>a</sup>

Different letters in the same row indicate significant differences according to Tukey's test ( $p < 0.05$ ). \* Values are significant at  $p < 0.05$ . (-): Not tested.

Abbreviation : DPPH, 1,1-diphenyl-2-picrylhydrazil ; FRAP, ferric reducing antioxidant power ; ICA, iron chementation assay

Table 2 Secondary metabolite composition of *T. lutea* microalgae cultured with different urea-based nanonutrients.

Culture	X1 : TCD (mg .g <sup>-1</sup> DW)	X2: TPC (mg GAE .g <sup>-1</sup> DW)	X3 :TCC (mg GluE . <sup>-1</sup> dw)
Control culture	25.20 ± 1.48 <sup>a</sup>	12.77 ± 0.82 <sup>a</sup>	31.12 ± 0.90 <sup>a</sup>
<u>A</u>	44.15 ± 2.48 <sup>d</sup>	19.10 ± 0.84 <sup>d</sup>	24.36 ± 0.30 <sup>f</sup>
<u>B</u>	31.25 ± 1.35 <sup>c</sup>	15.45 ± 0.66 <sup>c</sup>	25.00 ± 0.24 <sup>e</sup>
<u>C</u>	28.32 ± 1.48 <sup>b</sup>	14.29 ± 0.65 <sup>b</sup>	27.12 ± 0.32 <sup>d</sup>
<u>D</u>	28.44 ± 1.17 <sup>b</sup>	14.30 ± 0.60 <sup>b</sup>	26.15 ± 0.44 <sup>c</sup>
<u>E</u>	26.21 ± 1.22 <sup>a</sup>	13.82 ± 0.60 <sup>a,b</sup>	29.01 ± 0.82 <sup>b</sup>

Different letters in the same row indicate significant differences according to Tukey's test ( $p < 0.05$ ). \* Values are significant at  $p < 0.05$ . (-): Not tested.

Abbreviation : TCD, Total carotenoid; TPC, Total Phenolic content ; TCC, total carbohydrate content

### 3.3. Correlation of antioxidant activities with chemical profiles

Correlations between antioxidant activities and chemical profiles were established using two statistical methods: principal component analysis (PCA) and multiple linear regression (MLR) (Table S3 and Table S4). The principal component analysis, presented in Figure 2, showed that the antioxidant activity measured by the three methods (DPPH, FRAP, and ICA) is well correlated with the TCD and TPC. In contrast, the antioxidant activity did not show a significant relationship with TCC. Following the PCA results, a multiple linear regression was performed for the antioxidant activity using the two essential parameters: TCD and TPC. Table 3 presents the model equations coefficients of determination ( $R^2$ ), as well as the mean square errors (MSE) and root mean square errors (RMSE). According to the RLM results, the regression models for DPPH and FRAP perform very well, with coefficients of determination of 0.95 for DPPH and 0.96 for FRAP. On the other hand, the model for ICA, with a coefficient of determination of 0.74, does not show such a strong correlation. In general, both statistical tools PCA and RLM have allowed us to highlight significant correlations between the antioxidant activities of microalgae extracts and some chemical profiles. TCD and TPC contents are reliable indicators of antioxidant activity, especially for DPPH and FRAP methods. TCC, however, does not show a significant correlation with antioxidant activity [46-48].

Figure 2 Correlations between antioxidant activities and chemical profiles according to PCA.

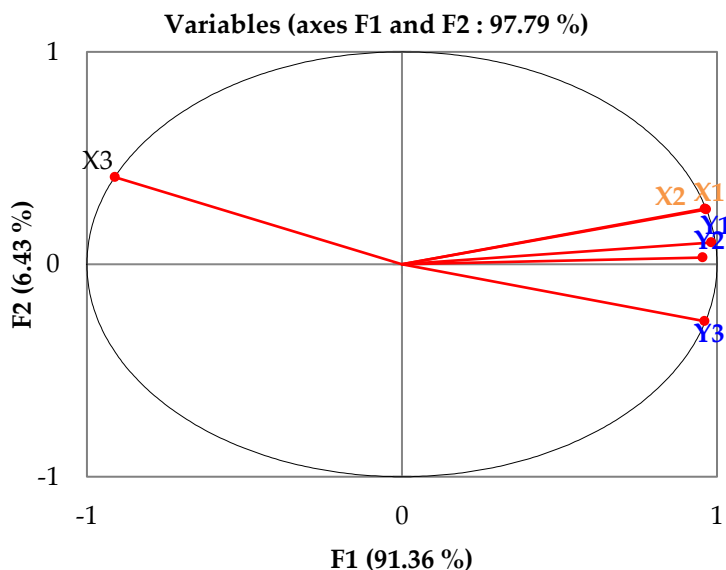


Table 3 Correlations between antioxidant activities and chemical profiles according to MLR.

Y1 : DPPH	Equation	$Y1 = -0.317 + (0.041 \times X1) - (0.004 \times X2)$
	R <sup>2</sup>	0.95
	MSE	0.008
	RMSE	0.092
Y2 : FRAP	Equation	$Y2 = -48.708 - (1.876 \times X1) + (7.269 \times X2)$
	R <sup>2</sup>	0.96
	MSE	0.416
	RMSE	0.645
Y3 : ICA	Equation	$Y3 = 11.095 + (0.014 \times X1) + (0.308 \times X2)$
	R <sup>2</sup>	0.74
	MSE	0.409
	RMSE	0.640

### 3.4. Correlation of antioxidant activities with molecular descriptors

Correlations between antioxidant activities and the 28 descriptors were established using two statistical methods: PCA and MLR (Table S5). The principal component analysis, presented in Figure 3, showed that the antioxidant activity measured by the three methods (DPPH, FRAP, and ICA) is well correlated with the six descriptors Z4 (N%), Z18 (Shape Coefficient), Z20 (Total Connectivity), Z23 (E<sub>LUMO</sub>), Z24 (Energy gap E<sub>GAP</sub>) and Z25 (Chemical hardness  $\eta$ ). On the other hand, the antioxidant activity did not show any significant relationship with the other molecular descriptors. Following these PCA results, a multiple linear regression was performed for the antioxidant activity using the five essential descriptors: Z4, Z18, Z20, Z23, Z24, and Z25. Table 4 presents the model equations coefficients of determination (R<sup>2</sup>) and the MSE and RMSE. According to the RLM results, the multiple linear regression models for the DPPH, FRAP, and ICA variables perfectly explain the data variance (with R<sup>2</sup> of 1 for each), and the prediction errors are extremely small. This may suggest that the model is very well adapted to the training data used.

The relationship between the antioxidant profile and chemical descriptors such as nitrogen percentage (N%), shape coefficient, total connectivity, energy of the highest occupied molecular orbital (ELUMO), E<sub>GAP</sub>, and chemical hardness ( $\eta$ ) can be interpreted by their influences on the structure and reactivity of molecules:

- The nitrogen percentage (N%) influences the formation of hydrogen bonds and the electron distribution, thus affecting the antioxidant activity [49].
- The shape coefficient evaluates the molecular geometry, where a specific shape can enhance the interaction with free radicals [50].
- Total connectivity is associated with structural complexity, where higher connectivity can stabilize free radicals via resonance mechanisms [51].
- The energy of the lowest unoccupied molecular orbital (E<sub>LUMO</sub>) reflects the ability of the molecule to accept electrons, which is essential for antioxidant reactions [52].
- The energy gap (E<sub>GAP</sub>) between occupied and unoccupied molecular orbitals indicates stability and reactivity, with a smaller E<sub>GAP</sub> favoring easy interaction with free radicals (Figure 4) [53].

- Finally, chemical hardness ( $\eta$ ) measures the resistance of a molecule to changing its electron density, with a lower hardness making the molecule more reactive and effective as an antioxidant [54].

Figure 3 Correlations between antioxidant activities and molecular descriptors according to PCA.

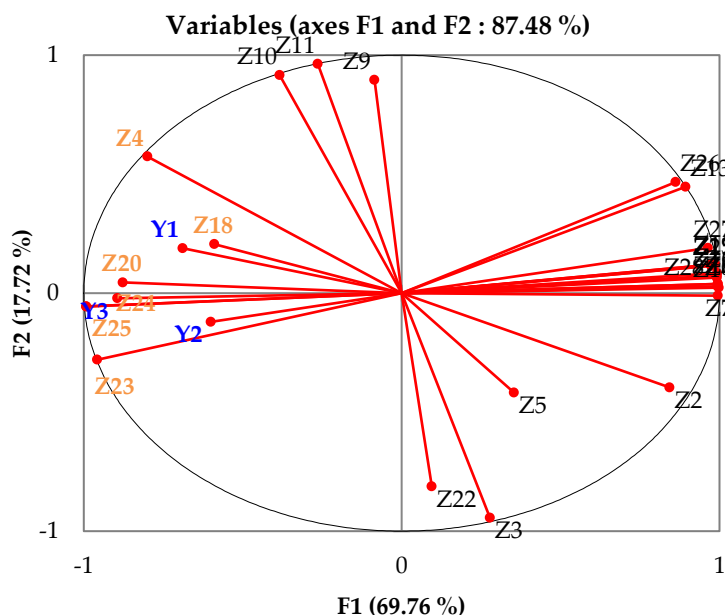
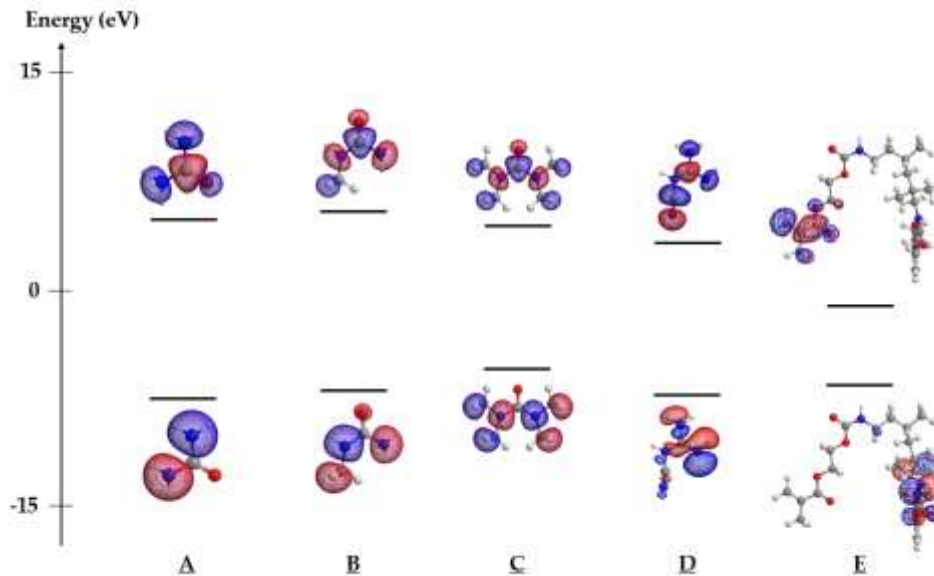


Table 4 Correlations between antioxidant activities and molecular descriptors according to MLR.

Y1 : DPPH	Equation	$Y1 = -1.9764 - (0.0128 \cdot Z4) + (0.2194 \cdot Z18) + (0.0538 \cdot Z20) - (0.1892 \cdot Z23) + (0.2037 \cdot Z24) + (0.1018 \cdot Z25)$
	R <sup>2</sup>	1
	MSE	$1.378 \times 10^{-30}$
	RMSE	$1.174 \times 10^{-15}$
Y2 : FRAP	Equation	$Y2 = -18.3791 - (0.1269 \cdot Z4) + (0.0924 \cdot Z18) + (0.3448 \cdot Z20) - (1.3669 \cdot Z23) + (1.6479 \cdot Z24) + (0.8240 \cdot Z25)$
	R <sup>2</sup>	1
	MSE	$3.179 \times 10^{-29}$
	RMSE	$5.638 \times 10^{-15}$
Y3 : ICA	Equation	$Y3 = 10.1280 - (0.0241 \cdot Z4) + (0.2123 \cdot Z18) + (0.0907 \cdot Z20) - (0.2930 \cdot Z23) + (0.4116 \cdot Z24) + (0.2058 \cdot Z25)$
	R <sup>2</sup>	1
	MSE	$3.787 \times 10^{-30}$
	RMSE	$1.946 \times 10^{-15}$

Figure 4. Distribution of molecular orbitals of different molecules of urea derivatives



### 3.5. Molecular Docking Study

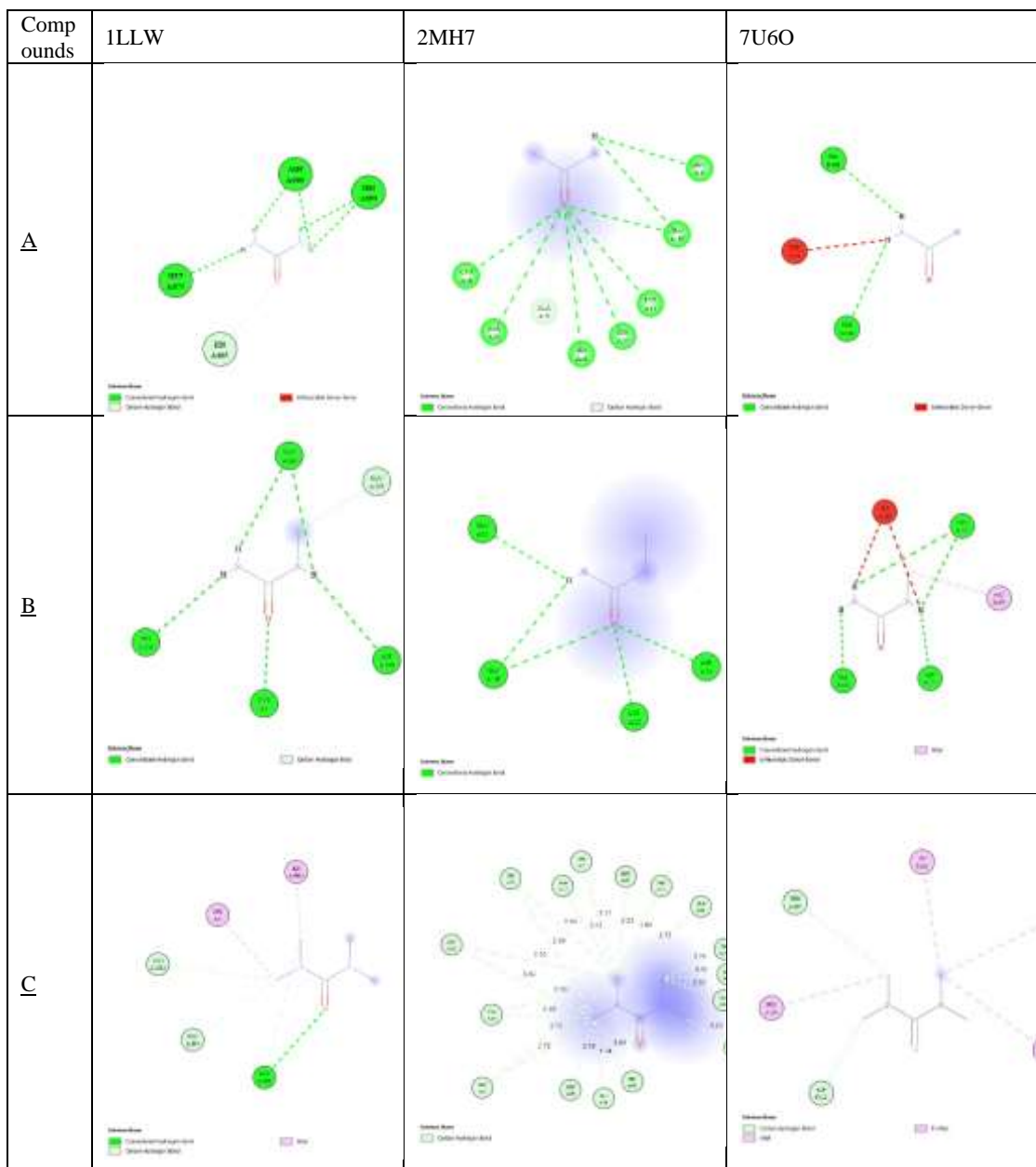
For molecular docking, urea and its derivatives (A, B, C, D, and E) as nitrogen ligands were studied with three proteins: 1LLW, 2MH7, and 7U6O. These proteins are essential for nitrogen management and fixation in various organisms, including microalgae:

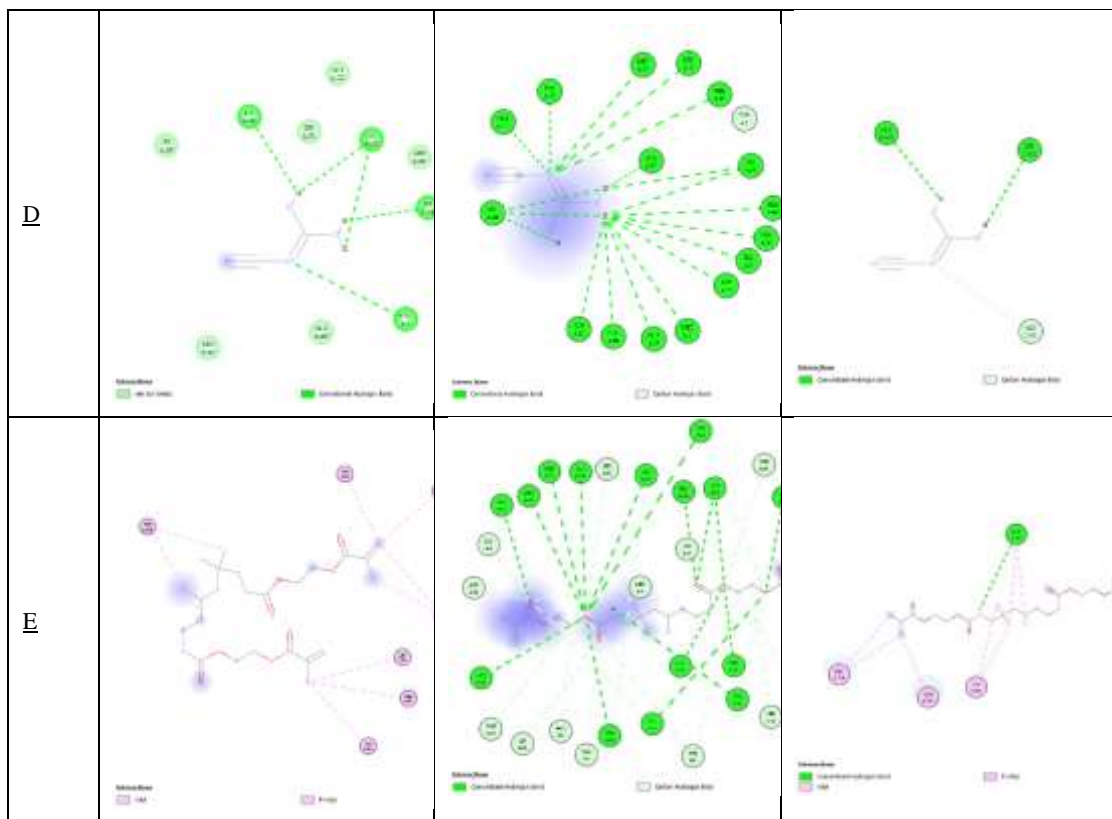
- Protein 2MH7 represents an iron-sulfur protein, acting as an electron carrier in many metabolic processes, including nitrogen fixation. This protein is important for transferring electrons to nitrogenase and other enzymes essential for nitrogen fixation [55].
- Protein 1LLW corresponds to Glutamate Synthase (GOGAT), an enzyme involved in the glutamic acid cycle. GOGAT synthesizes glutamine from glutamate and ammonia, playing an essential role in nitrogen metabolism in microalgae. This enzyme is essential for nitrogen metabolism, allowing cells to produce nitrogen compounds necessary for their growth and function [56].
- The 7U6O protein represents Glutamine Synthetase (GS), a key enzyme in nitrogen metabolism. GS catalyzes the synthesis of glutamine from glutamate and ammonia. It is involved in ammonia assimilation and regulation of nitrogen concentration in cells, playing a vital role in maintaining nitrogen balance and providing glutamine for various biosynthetic pathways [57].

Figure 5 presents the 2D images of the molecular docking of urea and its derivatives with the proteins 1LLW, 2MH7, and 7U6O involved in the mechanism of antioxidant activity. Preliminary analysis of this figure showed that conventional hydrogen bonding is indeed involved in most of the interactions between ligands and proteins. This proves the contribution to stability, specificity, orientation, and affinity of the interactions between ligands and their targets. These interactions are essential to accurately predict the complexes

formed and to design efficient ligands to develop new nitrogen-based nanonutrients, especially urea synthesis derivatives.

Figure 5 2D docked views of urea and its derivatives with proteins 1LLW, 2MH7, 7U6O involved in the mechanism of antioxidant activity.



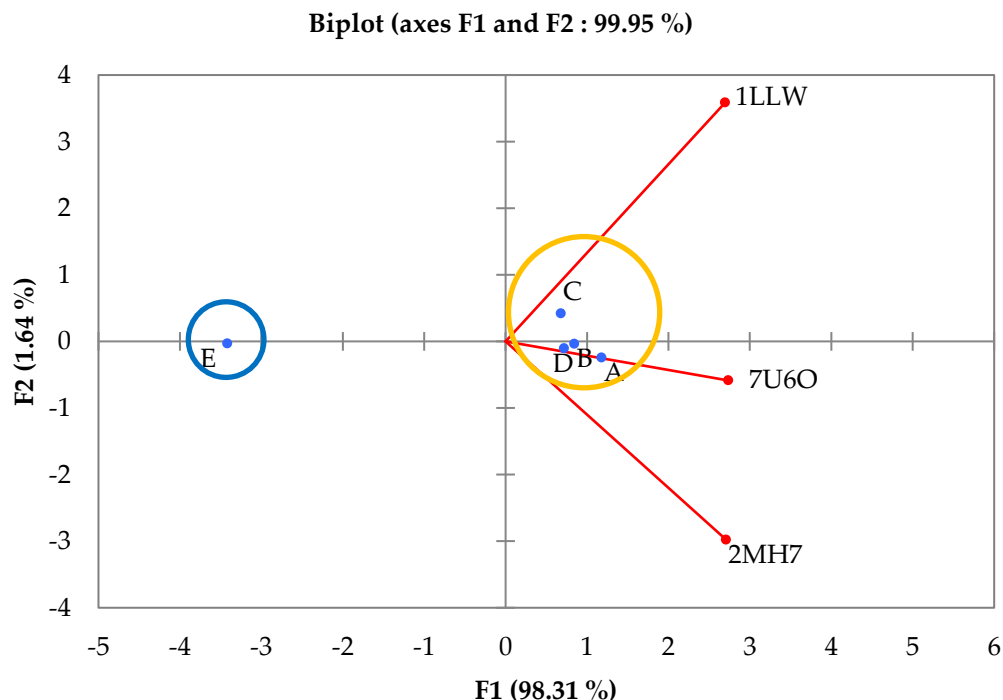


Binding Free Energy data for molecular dockings have been grouped in Table 5, and their correlations with urea and its derivatives are presented in Figure 5. PCA of molecular docking data revealed a significant correlation between most binding free energies of urea and its derivatives, particularly methylurea, tetramethylurea, and cyanoguanidine. These correlation results suggest uniformity and consistency in the molecular interactions studied. This can be interpreted as a positive sign indicating that ligands and targets have similar features that influence their binding energies [58].

Table 5 Binding Free Energy for molecular dockings.

Compounds	1LLW	2MH7	7U6O
<u>A</u>	-3.9	-17.5	-3.3
<u>B</u>	-3.9	-20.5	-3.7
<u>C</u>	-3.6	-25.4	-3.8
<u>D</u>	-4.1	-21.3	-3.7
<u>E</u>	-7.2	-48.9	-6.8

Figure 5 Correlations with PCA of all binding free energies for molecular dockings.



#### 4. Discussion

*T. lutea* culture enriched with urea-based nanonutrients was examined to assess its antioxidant potential and establish correlations with secondary metabolites as well as computational descriptors. This research explored the benefits of urea-based nanonutrients in enhancing the production of bioactive metabolites in microalgae using in vitro and in silico methods. *T. lutea*, marine microalgae known for their advanced biotechnological applications, were cultured in media containing different nanonutrients such as urea, methylurea, tetramethylurea, cyanoguanidine, and diurethane dimethacrylate at a concentration of 250 mM. A control without nanonutrients was also maintained for comparison. After cultivation, a series of maceration extractions were performed to isolate the bioactive compounds from the microalgae.

The antioxidant activity of the extracts was measured using three methods: DPPH, FRAP, and ICA. All extracts from nanonutrient-enriched cultures showed high antioxidant activities compared to the control. In addition, all extracts from nanonutrient-enriched cultures had higher total carotenoid and polyphenol contents compared to the control. On the other hand, the total carbohydrate content of all microalgae extracts decreased compared to the control, proving the positive effect of urea and its derivatives on antioxidant activity, carotenoids, and polyphenols, and the negative effect on carbohydrates [59].



Correlations between antioxidant activities and chemical profiles were established using two statistical methods: principal component analysis (PCA) and multiple linear regression (MLR). PCA showed that the antioxidant activity measured by the three methods (DPPH, FRAP and ICA) was well correlated with total carotenoid content (TCD) and total polyphenols (TPC). In contrast, antioxidant activity did not show a significant relationship with total carbohydrates (TCC). Following the PCA results, an MLR was performed for antioxidant activity using the two essential parameters: total carotenoid content (TCD) and total polyphenols (TPC). The regression models for DPPH and FRAP performed very well, while the model for ICA did not show such a strong correlation [60].

In addition, correlations between antioxidant activities and the 28 molecular descriptors were established using the same statistical methods. PCA showed that antioxidant activity measured by the three methods (DPPH, FRAP, and ICA) was well correlated with six descriptors: Z4 (N%), Z18 (Shape coefficient), Z20 (Total connectivity), Z23 (ELUMO), Z24 (EGAP energy gap) and Z25 (Chemical hardness  $\eta$ ). In contrast, antioxidant activity did not show any significant relationship with other molecular descriptors. Following these PCA results, an MLR was performed for antioxidant activity using the five essential descriptors: Z4, Z18, Z20, Z23, Z24, and Z25. The MLR results showed that multiple linear regression models for DPPH, FRAP, and ICA variables explained the variance of the data perfectly [61-62].

For molecular docking, urea and its derivatives were used as nitrogen ligands. Three proteins were involved in this computational approach: 1LLW, 2MH7, and 7U6O, which are essential for nitrogen management and fixation in various organisms, including microalgae. Analysis of molecular docking images of urea and its derivatives with proteins showed that conventional hydrogen bonding was indeed involved in most of the interactions between ligands and proteins. This proved the contribution to stability, specificity, orientation, and affinity of interactions between ligands and their targets [63-65]. These interactions were essential to accurately predict the complexes formed and to design efficient ligands in the development of new nitrogen-based nanonutrients, especially urea synthesis derivatives. Binding Free Energy data for molecular dockings were analyzed and correlated. The results demonstrated uniformity and consistency in the molecular interactions studied, indicating that ligands and targets had common features that similarly influenced their binding energies [66-67].

Our study demonstrated a high antioxidant potential of *T. lutea* cultures enriched with urea-based nanonutrients compared to the control, highlighting the effectiveness of nitrogen nanonutrients in improving the bioactive properties of microalgae. Statistical tools allowed to identify and quantify the relationships between antioxidant activities and chemical profiles as well as between molecular descriptors. Significant correlations were established between antioxidant activity and total carotenoid and total polyphenol contents, as well as with some molecular descriptors. In addition, the study of molecular docking of the interactions between urea and its derivatives with proteins essential for nitrogen management highlighted specific and stable interactions, confirming the relevance of these derivatives as effective nanonutrients.

Comparatively, the research of Zarrinmehr et al. (2020) [68] investigated the effect of

nitrogen concentration on the growth and biochemical composition of the microalga *Isochrysis galbana*. They found that decreasing nitrogen concentration decreased cell growth, pigments, and protein content. However, carbohydrates showed the highest value under total nitrogen deprivation. Polyunsaturated fatty acids (PUFAs) increased under sufficient nitrogen concentrations, while saturated fatty acids (SFAs) were higher under nitrogen deprivation. These results show that nitrogen concentration significantly affects the growth and biochemical composition of *I. galbana*, directly influencing secondary metabolites such as carbohydrates and fatty acids.

Coulombier et al. (2020) [69] investigated the effect of nitrogen availability on the antioxidant activity and carotenoid content of the microalga *Nephroselmis* sp. They observed increased carotenoid biosynthesis and higher antioxidant capacity under nitrogen-replete conditions. Pigment analyses revealed a specific photosynthetic system with siphonaxanthin-type light-harvesting complexes and high lutein and xanthophyll cycle pigment content. Peroxyl radical scavenging activities and total carotenoids were higher under nitrogen-replete conditions, while levels decreased under nitrogen-limiting or nitrogen-starved conditions. These results indicate that *Nephroselmis* sp. has significant potential as a natural source of antioxidants and pigments of interest, and that nitrogen availability plays a good role in the accumulation of these secondary metabolites.

Şirin et al. (2024) [70] explored the effects of nitrogen starvation on the growth and biochemical composition of *Dunaliella tertiolecta*, *Phaeodactylum tricornutum*, and *Nannochloropsis oculata*. Nitrogen starvation caused significant changes in the carbohydrate, protein, lipid, and fatty acid compositions of these microalgae. Under nitrogen stress, the carbohydrate content of *D. tertiolecta* increased by 59%, while the lipid level increased by 139% in *P. tricornutum* compared with the control groups. Nitrogen starvation also increased the oligosaccharide and polysaccharide contents of *D. tertiolecta* by a factor of 2.3 and 7.4 times, respectively. This increase is essential for the use of these microalgae as biodiesel feedstocks. In addition, nitrogen deprivation increased the contents of eicosapentaenoic acid in *N. oculata* and docosahexaenoic acid in *P. tricornutum*. These results demonstrate that nitrogen deprivation can increase the amounts of polyunsaturated fatty acids (PUFAs), eicosapentaenoic acid, docosahexaenoic acid, oligosaccharides, and polysaccharides, thereby significantly influencing secondary metabolites.

Manoyan et al. (2024) [71] investigated the effects of sulfur (S) and nitrogen (N) deprivation on photosynthetic pigments, polyphenols, photosystem activity, and hydrogen (H<sub>2</sub>) production in *Chlorella vulgaris* and *Parachlorella kessleri*. S and N deprivation decreased the growth of both cultures, accompanied by decreased photosynthetic pigments, PS II activity, and polyphenol synthesis. However, S and N deprivation increased H<sub>2</sub> production, with *P. kessleri* generating more H<sub>2</sub> than *C. vulgaris* under anaerobic conditions deprived of N and S. Inhibition of H<sub>2</sub> production by DCMU confirmed the involvement of PS II in this process. These results show that nitrogen deprivation can also influence the production of secondary metabolites such as hydrogen, a potential biofuel.

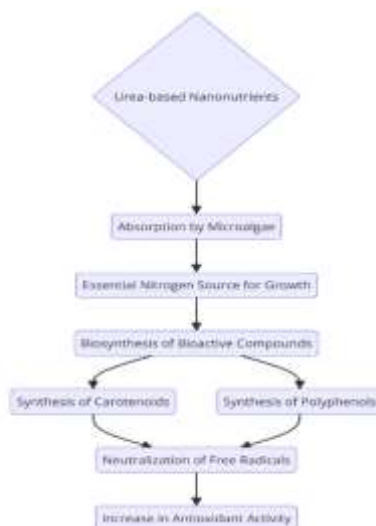
El-Sheekh et al. (2024) [72] studied the effects of salinity, nitrogen, and phosphorus deficiency on the growth and photosynthetic activity of the marine microalga *Dunaliella parva*. They found that nitrogen and phosphorus deficiency decreased the growth rate and

metabolic activities. Under salt stress combined with nitrogen deficiency, glycerin production increased, while glycerin synthesis decreased under 1 M NaCl salt stress and phosphorus deficiency. These results suggest that nitrogen deprivation, combined with other stresses, can modulate the production of secondary metabolites such as glycerin and antioxidant enzymes, playing an important role in the salinity tolerance mechanism of *D. parva*.

In conclusion, the effect of nitrogen on microalgae cultures and their secondary metabolites varies depending on species and culture conditions. Our study and comparative work show that nitrogen plays an essential element in regulating growth, biochemical composition and production of secondary metabolites, thus directly influencing the potential biotechnological applications of microalgae.

In conclusion, our study shows that nitrogen plays a fundamental role in microalgae cultivation, influencing their growth, biochemical composition and the production of bioactive molecules. For *Tisochrysis lutea*, the antioxidant potential is strongly correlated with the content of carotenoids and polyphenols, essential bioactive compounds in the neutralization of free radicals. In addition, some molecular descriptors, related to chemical and structural properties, have also shown a correlation with antioxidant activity, highlighting the importance of molecular composition in antioxidant efficacy. The use of urea-based nanonutrients enhances these effects by improving nitrogen management and increasing the production of carotenoids and polyphenols. These nanonutrients allow to stabilize key molecular interactions, which amplifies the antioxidant potential of *Tisochrysis lutea*. Thus, enriching cultures with these urea-based nanonutrients could not only optimize the antioxidant properties of this microalgae but also open new perspectives for its use in biotechnological applications. Our study highlights the importance of a thorough understanding of chemical interactions to maximize the bioactive capacities of microalgae (Figure 6).

Figure 6 Correlation mechanism between chemical composition and antioxidant potential of *Tisochrysis lutea* grown with urea-based nanonutrients.



## 5. Conclusion

*T. lutea* culture enriched with urea-based nanonutrients demonstrated remarkable antioxidant potential, with significant correlation with secondary metabolites, including carotenoids and polyphenols, as well as with molecular descriptors such as nitrogen percentage, shape coefficient, total connectivity,  $E_{LUMO}$ ,  $E_{GAP}$ , and  $\eta$ . Molecular interactions, studied via molecular docking, revealed specific and stable interactions, suggesting the potential antioxidant efficacy of urea derivatives as nanonutrients. The results obtained encourage further investigations to optimize the use of nitrogen-based nanonutrients, especially urea synthesis derivatives, to maximize the production of high value-added bioactive compounds. This research contributed to a better understanding of the mechanisms underlying interactions between nanonutrients and microalgae, opening opportunities for the development of new strategies for enriching microalgae cultures for biotechnological purposes. By combining *in vitro* and *in silico* approaches, this study provided a solid foundation for the future development of advanced algal biotechnologies, exploring and validating the complex interactions between microalgae and nanonutrients.

## References

1. Mishra, P.; Saini, P. Bioprospecting of Microalgae Derived Commercial Significant Compounds. In *Bioprospecting of Microbial Resources for Agriculture, Environment and Biochemical Industry*; Springer: Cham, Switzerland, 2024; pp. 75–85.
2. Jabłońska-Trypuć, A. Algae as Crop Plants Being a Source of Bioactive Ingredients of Pharmaceutical and Dietary Importance. *Agronomy* 2024, 14(5), 895.
3. Pehlivanov, I.; Gentsheva, G.; Nikolova, K.; Andonova, V. Some Applications of *Arthrospira platensis* and Algae in Pharmaceutical and Food Technologies. *Red* 2024, 29, 30.
4. Wang, M.; Morón-Ortiz, Á.; Zhou, J.; Benítez-González, A.; Mapelli-Brahm, P.; Meléndez-Martínez, A.J.; Barba, F.J. Effects of Pressurized Liquid Extraction with Dimethyl Sulfoxide on the Recovery of Carotenoids and Other Dietary Valuable Compounds from the Microalgae *Spirulina*, *Chlorella*, and *Phaeodactylum tricornutum*. *Food Chem.* 2023, 405, 134885.
5. Chaudhary, A.; et al. Dietary Supplementation of Microalgae Mitigates the Negative Effects of Heat Stress in Broilers. *Poultry Sci.* 2023, 102(10), 102958.
6. Ainane, T.; Abdoul-Latif, F.M.; El Yaagoubi, B.; Boujaber, N.; Oumaskour, K.; Ainane, A. *Nannochloropsis oculata* Microalga for Fertilization: Bioguided Fractionation of N-Hexane Extract by Stimulating Growth Activity for *Cucurbita moschata*. *Pharmacologyonline* 2021, 3, 1803–1809.
7. Rodriguez-Amaya, D.B.; Esquivel, P.; Meléndez-Martínez, A.J. Comprehensive Update on Carotenoid Colorants from Plants and Microalgae: Challenges and Advances from Research Laboratories to Industry. *Foods* 2023, 12(22), 4080.
8. Mohamed Abdoul-Latif, F.; Ainane, A.; Houmed Aboubaker, I.; Merito Ali, A.; Mohamed, H.; Jutur, P.P.; Ainane, T. Unlocking the Green Gold: Exploring the Cancer Treatment and the Other Therapeutic Potential of Fucoxanthin Derivatives from Microalgae. *Pharmaceuticals* 2024, 17(7), 960.
9. Abdoul-Latif, F.M.; Oumaskour, K.; Boujaber, N.; Ainane, A.; Mohamed, J.; Ainane, T. Formulations of a Cosmetic Product for Hair Care Based on Extract of the Microalga *Isochrysis galbana*: *In Vivo* and *In Vitro* Activities. *J. Anal. Sci. Appl. Biotechnol.* 2021, 3(1), 15–19.
10. Zou, L.G.; Zheng, D.L.; Yao, Y.T.; Wen, F.F.; Li, D.W.; Yang, Y.F.; Li, H.Y. Polyphenols Modulate Microalgae Metabolism with a Particular Increment in Lipid Accumulation. *Fuel Nanotechnology Perceptions* Vol. 20 No.4 (2024)

- 2023, 352, 129085.
11. Franco-Morgado, M.; Amador-Espejo, G.G.; Pérez-Cortés, M.; Gutiérrez-Urbe, J.A. Microalgae and Cyanobacteria Polysaccharides: Important Link for Nutrient Recycling and Revalorization of Agro-industrial Wastewater. *Appl. Food Res.* 2023, 3(1), 100296.
  12. Novoveská, L.; Nielsen, S.L.; Eroldoğan, O.T.; Haznedaroglu, B.Z.; Rinkevich, B.; Fazi, S.; Einarsson, H. Overview and Challenges of Large-Scale Cultivation of Photosynthetic Microalgae and Cyanobacteria. *Mar. Drugs* 2023, 21(8), 445.
  13. Udayan, A.; Sirohi, R.; Sreekumar, N.; Sang, B.I.; Sim, S.J. Mass Cultivation and Harvesting of Microalgal Biomass: Current Trends and Future Perspectives. *Bioresour. Technol.* 2022, 344, 126406.
  14. Wang, Z.; Cheng, J.; Sun, Y.; Jia, D.; Tang, Y.; Yang, W.; Cen, K. Comprehensive Understanding of Regulatory Mechanisms, Physiological Models, and Key Enzymes in Microalgal Cells Based on Various Concentrations of CO<sub>2</sub>. *Chem. Eng. J.* 2023, 454, 140233.
  15. Pandey, S.; Narayanan, I.; Vinayagam, R.; Selvaraj, R.; Varadavenkatesan, T.; Pugazhendhi, A. A Review on the Effect of Blue Green 11 Medium and Its Constituents on Microalgal Growth and Lipid Production. *J. Environ. Chem. Eng.* 2023, 11(3), 109984.
  16. Lacour, T.; Robert, E.; Lavaud, J. Sustained Xanthophyll Pigments-Related Photoprotective NPQ Is Involved in Photoinhibition in the Haptophyte *Tisochrysis lutea*. *Sci. Rep.* 2023, 13(1), 14694.
  17. Mohamadnia, S.; Tavakoli, O.; Faramarzi, M.A.; Shamsollahi, Z. Production of Fucoxanthin by the Microalga *Tisochrysis lutea*: A Review of Recent Developments. *Aquaculture* 2020, 516, 734637.
  18. Mohamadnia, S.; Tavakoli, O.; Faramarzi, M.A. Enhancing Production of Fucoxanthin by the Optimization of Culture Media of the Microalga *Tisochrysis lutea*. *Aquaculture* 2021, 533, 736074.
  19. Liang, L.; Wang, Z.; Ding, Y.; Li, Y.; Wen, X. Protein Reserves Elucidate the Growth of Microalgae under Nitrogen Deficiency. *Algal Res.* 2023, 75, 103269.
  20. Khan, S.; Das, P.; Thaher, M.I.; AbdulQuadir, M.; Mahata, C.; Al Jabri, H. Utilization of Nitrogen-Rich Agricultural Waste Streams by Microalgae for the Production of Protein and Value-Added Compounds. *Curr. Opin. Green Sustainable Chem.* 2023, 41, 100797.
  21. Truong, T.Q.; Park, Y.J.; Winarto, J.; Huynh, P.K.; Moon, J.; Choi, Y.B.; Kim, S.M. Understanding the Impact of Nitrogen Availability: A Limiting Factor for Enhancing Fucoxanthin Productivity in Microalgae Cultivation. *Mar. Drugs* 2024, 22(2), 93.
  22. Salgado, E.M.; Esteves, A.F.; Gonçalves, A.L.; Pires, J.C. Microalgal Cultures for the Remediation of Wastewaters with Different Nitrogen to Phosphorus Ratios: Process Modelling Using Artificial Neural Networks. *Environ. Res.* 2023, 231, 116076.
  23. Khanzada, Z.T.; Övez, S. Growing Fresh Water Microalgae in High Ammonium Landfill Leachate. *Am. J. Mech. Appl.* 2018, 6(2), 50–61.
  24. Gutierrez, J.; Kwan, T.A.; Zimmerman, J.B.; Peccia, J. Ammonia Inhibition in Oleaginous Microalgae. *Algal Res.* 2016, 19, 123–127.
  25. Moreno-Marín, F.; Vergara, J.J.; Pérez-Llorens, J.L.; Pedersen, M.F.; Brun, F.G. Interaction between Ammonium Toxicity and Green Tide Development over Seagrass Meadows: A Laboratory Study. *PLoS ONE* 2016, 11(4), e0152971.
  26. Eze, C.N.; Aoyagi, H.; Ogbonna, J.C. Simultaneous Accumulation of Lipid and Carotenoid in Freshwater Green Microalgae *Desmodesmus subspicatus* LC172266 by Nutrient Replete Strategy under Mixotrophic Condition. *Korean J. Chem. Eng.* 2020, 37, 1522–1529.
  27. Minyuk, G.; Sidorov, R.; Solovchenko, A. Effect of Nitrogen Source on the Growth, Lipid, and Valuable Carotenoid Production in the Green Microalga *Chromochloris zofingiensis*. *J. Appl. Phycol.* 2020, 32, 923–935.
  28. Molina-Miras, A.; Abreu, A.C.; Rosales, L.L.; Cerón-García, M.C.; Sánchez-Mirón, A.;

- Fernández, I.; García-Camacho, F. A Step Forward in Sustainable Pesticide Production from *Amphidinium carterae* Biomass via Photobioreactor Cultivation with Urea as a Nitrogen Source. *Bioresour. Technol.* 2023, 387, 129643.
29. Rosa, R.M.; Machado, M.; Vaz, M.G.M.V.; Lopes-Santos, R.; do Nascimento, A.G.; Araújo, W.L.; Nunes-Nesi, A. Urea as a Source of Nitrogen and Carbon Leads to Increased Photosynthesis Rates in *Chlamydomonas reinhardtii* under Mixotrophy. *J. Biotechnol.* 2023, 367, 20–30.
  30. Zhou, H.; Wang, J.; Zhang, Z.; Lan, C.Q. High Cell Density Culture of Microalgae in Horizontal Thin-Layer Algal Reactor: Modeling of Light Attenuation and Cell Growth Kinetics. *Chem. Eng. J.* 2024, 154175.
  31. Figueroa-Torres, G.M.; Pittman, J.K.; Theodoropoulos, C. Optimisation of Microalgal Cultivation via Nutrient-Enhanced Strategies: The Biorefinery Paradigm. *Biotechnol. Biofuels* 2021, 14, 1–16.
  32. Darvehei, P.; Bahri, P.A.; Moheimani, N.R. Model Development for the Growth of Microalgae: A Review. *Renew. Sustain. Energy Rev.* 2018, 97, 233–258.
  33. Mohamed Abdoul-Latif, F.; Ainane, A.; Aboubaker, I.H.; Houssein Kidar, B.; Mohamed, J.; Lemrani, M.; Ainane, T. *Ericaria amentacea* Algae Extracts: A Sustainable Approach for the Green Synthesis of Silver Oxide Nanoparticles and Their Effectiveness against Leishmaniasis. *Processes* 2023, 11(11), 3227.
  34. Ma, R.; Cao, T.; An, H.; Yu, S.; Ji, H.; Liu, A. Extraction, Purification, Structure, and Antioxidant Activity of Polysaccharide from *Rhodiola rosea*. *J. Mol. Struct.* 2023, 1283, 135310.
  35. Rumpf, J.; Burger, R.; Schulze, M. Statistical Evaluation of DPPH, ABTS, FRAP, and Folin-Ciocalteu Assays to Assess the Antioxidant Capacity of Lignins. *Int. J. Biol. Macromol.* 2023, 233, 123470.
  36. Eruygur, N.; Tuzcu, N.; Tugay, O.; Yilmaz, M.A.; Cakir, O. Phytochemical Characterization and Biological Activities of *Inula viscosa* L. Aiton: A Promising Plant from Turkey. *Int. J. Environ. Health Res.* 2024, 1–14.
  37. Liang, Z.; Zhang, P.; Xiong, Y.; Johnson, S.K.; Fang, Z. Phenolic and Carotenoid Characterization of the Ethanol Extract of an Australian Native Plant *Haemodorum spicatum*. *Food Chem.* 2023, 399, 133969.
  38. Sanou, A.; Konaté, K.; Kabakde, K.; Dakuyo, R.; Bazié, D.; Hemayoro, S.; Dicko, M.H. Modelling and Optimisation of Ultrasound-Assisted Extraction of Roselle Phenolic Compounds Using the Surface Response Method. *Sci. Rep.* 2023, 13(1), 358.
  39. Rašeta, M.; Kebert, M.; Mišković, J.; Kostić, S.; Kaišarević, S.; Stilinović, N.; Karaman, M. *Ganoderma pfeifferi* Bres. and *Ganoderma resinaceum* Boud. as Potential Therapeutic Agents: A Comparative Study on Antiproliferative and Lipid-Lowering Properties. *J. Fungi* 2024, 10(7).
  40. Lanez, E.; Kedadra, A.; Lanez, T.; Adaika, A.; Zegheb, N. In Vitro Antioxidant Activity, QSAR, In Silico Toxicity Prediction, Molecular Docking Studies, and Molecular Dynamics of a Series of N-Ferrocenylmethylanilines as Potent Antioxidant Agents. *J. Organomet. Chem.* 2024, 123284.
  41. Li, H.; Lin, G.; Liang, Z.; Li, Y.; Zhang, R. Investigative on the Molecular Mechanism of Novel Antioxidation Peptides by 3D-QSAR, In Vitro Assay and MD Simulations. *J. Mol. Struct.* 2024, 1295, 136808.
  42. Idrovo-Encalada, A.M.; Rojas, A.M.; Fissore, E.N.; Tripaldi, P.; Pis Diez, R.; Rojas, C. Chemoinformatic Modelling of the Antioxidant Activity of Phenolic Compounds. *J. Sci. Food Agric.* 2023, 103(10), 4867–4875.
  43. Mohamed Abdoul-Latif, F.; Ainane, A.; Merito, A.; Houmed Aboubaker, I.; Mohamed, H.; Cherroud, S.; Ainane, T. The Effects of Khat Chewing among Djiboutians: Dental Chemical

- Studies, Gingival Histopathological Analyses and Bioinformatics Approaches. *Bioengineering* 2024, 11(7), 716.
44. Shahidi, F.; Dissanayaka, C.S. Phenolic-Protein Interactions: Insight from In-Silico Analyses–A Review. *Food Prod. Process. Nutr.* 2023, 5(1), 2.
  45. Sun, X.; Yu, Y.; Saleh, A.S.; Yang, X.; Ma, J.; Li, W.; Wang, Z. Understanding Interactions among Flavor Compounds from Spices and Myofibrillar Proteins by Multi-Spectroscopy and Molecular Docking Simulation. *Int. J. Biol. Macromol.* 2023, 229, 188–198.
  46. Santiago-Díaz, P.; Rivero, A.; Rico, M.; Gómez-Pinchetti, J.L. Characterization of Novel Selected Microalgae for Antioxidant Activity and Polyphenols, Amino Acids, and Carbohydrates. *Mar. Drugs* 2021, 20(1), 40.
  47. Kourouma, V.; Mu, T.H.; Zhang, M.; Sun, H.N. Comparative Study on Chemical Composition, Polyphenols, Flavonoids, Carotenoids and Antioxidant Activities of Various Cultivars of Sweet Potato. *Int. J. Food Sci. Technol.* 2020, 55(1), 369–378.
  48. Moloto, M.R.; Phan, A.D.T.; Shai, J.L.; Sultanbawa, Y.; Sivakumar, D. Comparison of Phenolic Compounds, Carotenoids, Amino Acid Composition, In Vitro Antioxidant and Anti-Diabetic Activities in the Leaves of Seven Cowpea (*Vigna unguiculata*) Cultivars. *Foods* 2020, 9(9), 1285.
  49. Parcheta, M.; Świsłocka, R.; Orzechowska, S.; Akimowicz, M.; Choińska, R.; Lewandowski, W. Recent Developments in Effective Antioxidants: The Structure and Antioxidant Properties. *Materials* 2021, 14(8), 1984.
  50. Rasulev, B.F.; Abdullaev, N.D.; Syrov, V.N.; Leszczynski, J. A Quantitative Structure-Activity Relationship (QSAR) Study of the Antioxidant Activity of Flavonoids. *QSAR Comb. Sci.* 2005, 24(9), 1056–1065.
  51. Rastija, V.; Medić-Šarić, M. QSAR Study of Antioxidant Activity of Wine Polyphenols. *Eur. J. Med. Chem.* 2009, 44(1), 400–408.
  52. Reis, M.; Lobato, B.; Lameira, J.; Santos, A.S.; Alves, C.N. A Theoretical Study of Phenolic Compounds with Antioxidant Properties. *Eur. J. Med. Chem.* 2007, 42(4), 440–446.
  53. Cai, W.; Chen, Y.; Xie, L.; Zhang, H.; Hou, C. Characterization and Density Functional Theory Study of the Antioxidant Activity of Quercetin and Its Sugar-Containing Analogues. *Eur. Food Res. Technol.* 2014, 238, 121–128.
  54. Waki, T.; Nakanishi, I.; Matsumoto, K.I.; Kitajima, J.; Chikuma, T.; Kobayashi, S. Key Role of Chemical Hardness to Compare 2,2-Diphenyl-1-Picrylhydrazyl Radical Scavenging Power of Flavone and Flavonol O-Glycoside and C-Glycoside Derivatives. *Chem. Pharm. Bull.* 2012, 60(1), 37–44.
  55. Xu, X.M.; Møller, S.G. Iron–Sulfur Clusters: Biogenesis, Molecular Mechanisms, and Their Functional Significance. *Antioxid. Redox Signal.* 2011, 15(1), 271–307.
  56. Liao, H.S.; Chung, Y.H.; Hsieh, M.H. Glutamate: A Multifunctional Amino Acid in Plants. *Plant Sci.* 2022, 318, 111238.
  57. Kong, L.; Xie, Y.; Hu, L.; Si, J.; Wang, Z. Excessive Nitrogen Application Dampens Antioxidant Capacity and Grain Filling in Wheat as Revealed by Metabolic and Physiological Analyses. *Sci. Rep.* 2017, 7(1), 43363.
  58. Saha, S.; Panieri, E.; Suzen, S.; Saso, L. The Interaction of Flavonols with Membrane Components: Potential Effect on Antioxidant Activity. *J. Membr. Biol.* 2020, 253, 57–71.
  59. Nilsson, J.; Olsson, K.; Engqvist, G.; Ekvall, J.; Olsson, M.; Nyman, M.; Åkesson, B. Variation in the Content of Glucosinolates, Hydroxycinnamic Acids, Carotenoids, Total Antioxidant Capacity and Low-Molecular-Weight Carbohydrates in Brassica Vegetables. *J. Sci. Food Agric.* 2006, 86(4), 528–538.
  60. Mokrani, A.; Cluzet, S.; Madani, K.; Pakina, E.; Gadzhikurbanov, A.; Mesnil, M.; Richard, T. HPLC-DAD-MS/MS Profiling of Phenolics from Different Varieties of Peach Leaves and Evaluation of Their Antioxidant Activity: A Comparative Study. *Int. J. Mass Spectrom.* 2019,

- 445, 116192.
61. Tao, Y.; Zhang, H.; Wang, Y. Revealing and Predicting the Relationship between the Molecular Structure and Antioxidant Activity of Flavonoids. *LWT* 2023, 174, 114433.
  62. Shi, Y. Support Vector Regression-Based QSAR Models for Prediction of Antioxidant Activity of Phenolic Compounds. *Sci. Rep.* 2021, 11(1), 8806.
  63. Nedić, O.; Penezić, A.; Minić, S.; Radomirović, M.; Nikolić, M.; Ćirković Veličković, T.; Gligorijević, N. Food Antioxidants and Their Interaction with Human Proteins. *Antioxidants* 2023, 12(4), 815.
  64. Shahidi, F.; Dissanayaka, C.S. Phenolic-Protein Interactions: Insight from In-Silico Analyses—A Review. *Food Prod. Process. Nutr.* 2023, 5(1), 2.
  65. Nepovimova, E.; Korabecny, J.; Dolezal, R.; Babkova, K.; Ondrejicek, A.; Jun, D.; Kuca, K. Tacrine–Trolox Hybrids: A Novel Class of Centrally Active, Nonhepatotoxic Multi-Target-Directed Ligands Exerting Anticholinesterase and Antioxidant Activities with Low In Vivo Toxicity. *J. Med. Chem.* 2015, 58(22), 8985–9003.
  66. Sumrra, S.H.; Hassan, A.U.; Zafar, M.N.; Shafqat, S.S.; Mustafa, G.; Zafar, M.N.; Imran, M. Metal Incorporated Sulfonamides as Promising Multidrug Targets: Combined Enzyme Inhibitory, Antimicrobial, Antioxidant and Theoretical Exploration. *J. Mol. Struct.* 2022, 1250, 131710.
  67. Kostova, I.; Balkansky, S. Metal Complexes of Biologically Active Ligands as Potential Antioxidants. *Curr. Med. Chem.* 2013, 20(36), 4508–4539.
  68. Amic, D.; Davidovic-Amic, D.; Beslo, D.; Rastija, V.; Lucic, B.; Trinajstic, N. SAR and QSAR of the Antioxidant Activity of Flavonoids. *Curr. Med. Chem.* 2007, 14(7), 827–845.
  69. Zarrinmehr, M.J.; Farhadian, O.; Heyrati, F.P.; Keramat, J.; Koutra, E.; Kornaros, M.; Daneshvar, E. Effect of Nitrogen Concentration on the Growth Rate and Biochemical Composition of the Microalga, *Isochrysis galbana*. *Egypt. J. Aquat. Res.* 2020, 46(2), 153–158.
  70. Şirin, P.A.; Serdar, S. Effects of Nitrogen Starvation on Growth and Biochemical Composition of Some Microalgae Species. *Folia Microbiol.* 2024, 1–14.
  71. Manoyan, J.; Hakobyan, L.; Samovich, T.; Kozel, N.; Sahakyan, N.; Muravitskaya, H.; Gabrielyan, L. Comparison of Sulfur and Nitrogen Deprivation Effects on Photosynthetic Pigments, Polyphenols, Photosystems Activity and H<sub>2</sub> Generation in *Chlorella vulgaris* and *Parachlorella kessleri*. *Int. J. Hydrogen Energy* 2024, 59, 408–418.
  72. Mostafa, E.S.; Dewidar, S.; Hamad, A.; Abu-elsaoud, A.M.; Alharbi, M.; Elkelish, A. Effect of Salinity, Nitrogen and Phosphorus Stresses on Growth and Photosynthetic Activity of the Marine Microalga *Dunaliella parva*. *Notul. Bot. Horti Agrobot. Cluj-Napoca* 2024, 52(1), 13426–13426.